



Spatial variability of dust concentration and deposition around an industrial port in South Africa emphasises the complexity of sources and transport

Heleen C. Vos^{1,2} · Kaukuraee I. Kanguehi¹ · René Toesie³ · Frank D. Eckardt⁴ · Grant Ravenscroft⁵ · Susanne Fietz¹

Received: 31 December 2023 / Accepted: 30 April 2024
© The Author(s) 2024

Abstract

The port and industrial zone of Saldanha Bay in South Africa accommodates activities related to the transport, processing, and production of commodities such as iron ore, manganese ore, and steel. The visible emission of dust from this area raised concerns for public health and to address this, the municipality has monitored the fine particulate matter (PM_{2.5}) concentration and dust deposition since 2015. Here, this monitoring data served to assess spatial and temporal changes and to evaluate the potential contribution of industrial and meteorological processes to these changes. We observed high temporal variability in both PM_{2.5} concentration and dust deposition, and high spatial variation in dust depositions. Dust originated from local sources such as industry and traffic, but industrial activities could not explain the observed spatial variability, and concentration and deposition fluxes did not significantly increase over the years despite the extension of industrial activities. Meteorological factors such as rain, wind speed, wind direction, as well as topography exerted an important influence, but could also only partially explain the observed variability in both dust concentration and deposition. Furthermore, the PM_{2.5} concentration and dust deposition are not significantly correlated, which highlights the challenges in appropriate dust monitoring. It follows that such monitoring efforts, though meeting national standards, require improvement to assess risks accurately. Our study illustrates that in areas with such high complexity of industrial activities, the high variability of dust load and deposition must be considered to evaluate implications for public and environmental health, adherence to guidelines, and mitigation strategies.

Keywords Air pollution · Dust deposition · PM_{2.5} concentration · Public health · Mining

Introduction

Dust emission, transport, and deposition play several critical roles, affecting land degradation, climate, the environment and public health. For example, the removal of fine particles can deplete emitting surfaces in nutrients, clay, and silt (Bridges and Oldeman 1999). Furthermore, through cloud condensation and direct radiative forcing, suspended particles can modulate regional (Marcella and Eltahir 2014; Pan et al. 2018) and global climate (Mahowald et al. 2014; Samset et al. 2018). The depositional of dust can lead to an enrichment in nutrients and fines and therefore play crucial roles in ocean fertilization (Grantz et al. 2003; Dansie et al. 2017). Any toxic particles present in dust can also negatively affect the environment (Farmer 1993; Paytan et al. 2009). Lastly, dust can strongly affect public health, which is a phenomenon that has attracted attention from the

✉ Heleen C. Vos
heleenvos@sun.ac.za

¹ Department of Earth Sciences, University of Stellenbosch, Stellenbosch 7600, South Africa

² BIOGRIP Water and Soil Node, University of Stellenbosch, Stellenbosch 7600, South Africa

³ Municipality of Saldanha Bay, Vredenburg 7380, South Africa

⁴ Department of Environmental & Geographical Science, University of Cape Town, Cape Town 7700, South Africa

⁵ Argos Scientific Pty Ltd., Cape Town 7405, South Africa

health sector (Li et al. 2019; Pandey et al. 2021). The World Health Organisation (WHO) estimates that in 2019, 4.2 million people died prematurely due to outdoor air pollution, whereby 89% of these deaths occurred in middle- and low-income countries (WHO 2021). The exposure to air pollution and the number of deaths from outdoor air pollution has decreased in most South American, North American, and European countries during the last 30 years, but increased in Asian and African countries (Ritchie and Roser 2019). In response to this global threat, studies have focussed on the precise effects of dust on human health and the characteristics of this effect from different dust sources.

The impact of dust on human health depends on both the concentration and the physical and chemical characteristics of the dust particles (Entwistle et al. 2019; Al-Swadi et al. 2022), which are determined by their emitting source (Csavina et al. 2012; Goudie 2013; Bauer et al. 2019; Querol et al. 2019). Dust sources can be divided into natural dust sources, such as dunes, ephemeral rivers and lakes, and shrublands, and anthropogenic dust sources, which mainly consist of agricultural areas, mining areas, fires, and industrial processes (Koch et al. 2007; Ginoux et al. 2012; Xia et al. 2022). Generally, anthropogenic dust has a relatively high negative impact on public health and the environment (Csavina et al. 2012; Bauer et al. 2019; Xia et al. 2022) since dust from these sources often consists of finer particles and contains contaminants such as heavy metals, pesticides, and pathogens (Landrigan and Baker 1981; McCartor and Becker 2010; Csavina et al. 2011; Salawu-Rotimi et al. 2021).

Csavina et al. (2012) estimated that from the variety of anthropogenic sources, activities related to mining and the processing of these mining materials have the highest potential risk to human and environmental health, and many studies have addressed this negative impact (Zheng et al. 2010; Csavina et al. 2011; Al-Swadi et al. 2022). Hereby, significant amounts of dust can not only be emitted by quarries, but also by secondary mining processes, such as crushing, grinding, separation, smelting, and transport (Csavina et al. 2011; Kristensen et al. 2015). Such diversity and spatial variance in mining and mining-related industrial activities need to be considered when addressing the health and environmental impact.

The port at Saldanha Bay is situated on the west coast of South Africa and is an important port for the transport of mining materials and includes an industrial zone that is responsible for processing this material. In this area, 55.2 million tons of iron ore and 4.7 million tons of magnesium ore have been stored, processed, and transported in 2021/2022 (AEC 2022). Furthermore, lead, copper, zinc, and steel, which include galvanized steel, have been produced in this area. In smaller amounts, titanium slag, rutile,

and crude iron are processed and transported, along with phosphate from nearby phosphate mines (AEC 2022). The Saldanha Bay Municipality furthermore includes densely populated residential areas and key national protected areas, making it a region with a high diversity of land use.

The production and export of materials generally expanded since early 2000 (AEC 2022), despite the closure of one of the steel plants in February 2020 and the fact that the general economy has been affected by the COVID-19 lockdown in 2020 and 2021. Especially the export of manganese ore and lead increased rapidly over the last eight years. Future development includes increasing the storage and handling capacity of iron ore, expanding the rail and port, increasing the industrial capacity, developing biofuel and gas production facilities, and a general expansion of the industrial activities.

The high quantity of mining material transported, stored, and processed in this area resulted in the visible emission of dust. The dust emitted from the iron ore can be observed in the area as a “red dust plume” (AEC 2022). Furthermore, the rail and road transport of mining materials has been acknowledged as a possible source of dust (DEA&DP 2019; Saldanha Bay Municipality 2023). The dust in this region has raised concerns about its impact on public health. It should furthermore be considered that the smaller, less visible particles from transport and smelting activities could also be harmful. Lastly, the dust could impact the environment, either by depositing nutrients or toxic particles in the surrounding areas (AEC 2022).

To support health risk assessments in the residential areas surrounding the port, the Saldanha Bay Municipality installed dust monitoring equipment in 2015. This equipment consists of a fine particulate matter (PM_{2.5}) monitoring station and several dust buckets and aims at addressing whether the National Ambient Air Quality Standards (NAAQS) have been crossed in these areas. The data that was produced from this monitoring has not been further analysed on any temporal and spatial patterns and any anthropogenic influences on these patterns. This knowledge would be of importance for understanding the future development of the area and developing any possible mitigation strategies.

This study aims to understand the spatial and temporal variations of the dust emission around Saldanha Bay, the specific sources of dust, and any possible natural and anthropogenic drivers behind this variation. To do so, dust monitoring data from 2015 to 2022 by the Saldanha Bay Municipality will be analysed in combination with weather data. We will furthermore address the potential impact of the dust on public health and determine the possible impacted environmental areas. These results can function as an initial understanding of the high health-risk areas of this region

and temporal variation caused by meteorological effects. It will furthermore give insight into the effects of expanding industrial activities on the dust load in the area.

Methods

Study area

The Saldanha Bay Municipality is located on the west coast of South Africa and holds the Saldanha Bay port and the surrounding industrial area (Fig. 1). The Saldanha Bay port area is roughly 5 km long and 5 km wide and hosts the dry bulk stockpile, where iron ore is being stored, the multipurpose and iron ore terminal, and the dry and liquid bulk terminal. The industrial area surrounding it, called the Besaansklip Industrial Area, is much larger and includes, among others, various smelters and steel plants, the industrial development zone, and a gravel quarry. South of the port area lies the West Coast National Park, part of the UNESCO Cape West Coast Biosphere Reserve. Two towns are in proximity to the industrial area: Saldanha and Vredenburg, where respectively 28,000 and 38,000 people live. In total, including informal settlements, around 123,000 people live in this municipality (SEP 2021).

Climate and weather monitoring

Daily weather data from 2015 to 2022 has been provided by the South African Weather Service (SAWS) from a climate station at Langebaanweg (Fig. 1). This data includes

the hourly rainfall, wind velocity, and wind direction. The study area received an average annual rainfall of 234 mm between 2015 and 2022 and is characterised by winter rainfall (Fig. 2). The winds generally come from south to southwest, albeit occasionally winds come from north to northeast (Fig. 2). The wind velocity is generally higher during winter with a more pronounced north-northeastern wind direction during this period (Figures S1 and S2). From 2015 to 2022, the wind velocity distribution did not significantly change (Figures S2 and S3).

Dust monitoring

PM_{2.5} monitoring

Ambient concentrations of particulates of less than 2.5 µm in diameter (PM_{2.5}) were measured in the town of Saldanha (Fig. 1). The PM_{2.5} content is generally used to assess the impact of dust on public health (WHO 2016, 2021; Cui et al. 2019; Khreis et al. 2023). The PM_{2.5} concentration was measured according to the South African Ambient Air Quality Standards methods (DEA 2013) using a Tapered Element Oscillating Microbalance (TEOM). The concentration was measured at hourly intervals from January 2015 to September 2018. Due to vandalization, no measurements were performed after this period. To further analyse the measured PM_{2.5} concentration and to compare the data to national and international health standards (see Sect. 2.3.3), the daily average of the PM_{2.5} concentration was calculated as the sum of the hourly measurements divided by the duration.

Fig. 1 Map of southern Africa (a), Saldanha Bay located in the West Coast District (b), and locations of installed monitoring equipment (c). See c for legend and Sect. 2.3.3. for monitoring station abbreviation. Credits: Esri South Africa, Esri, HERE Garmin, Foursquare, METI/NASA, and USGS

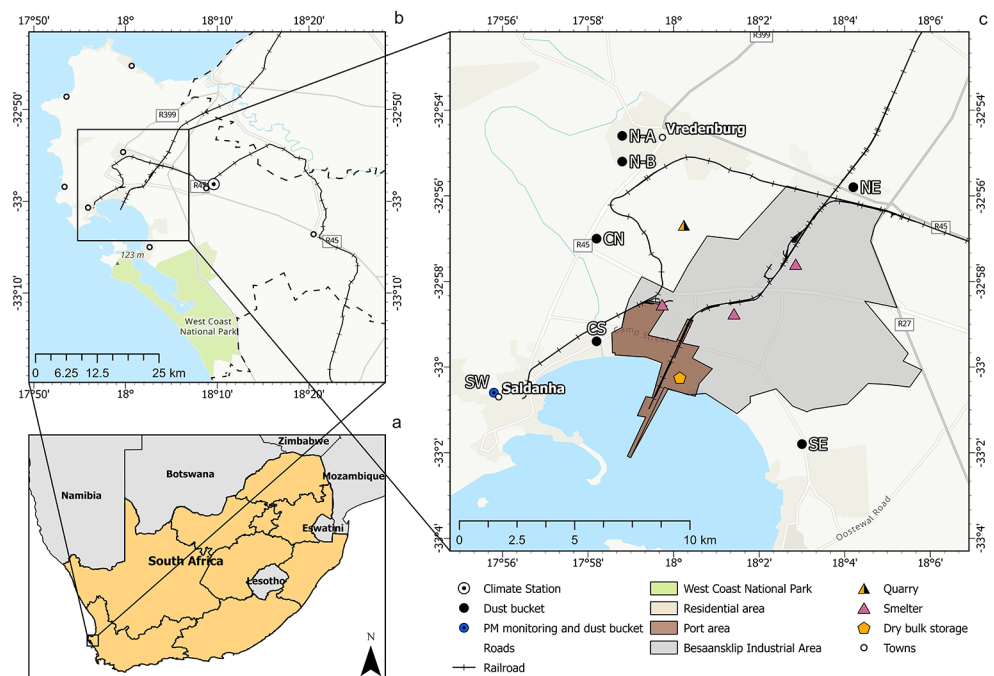
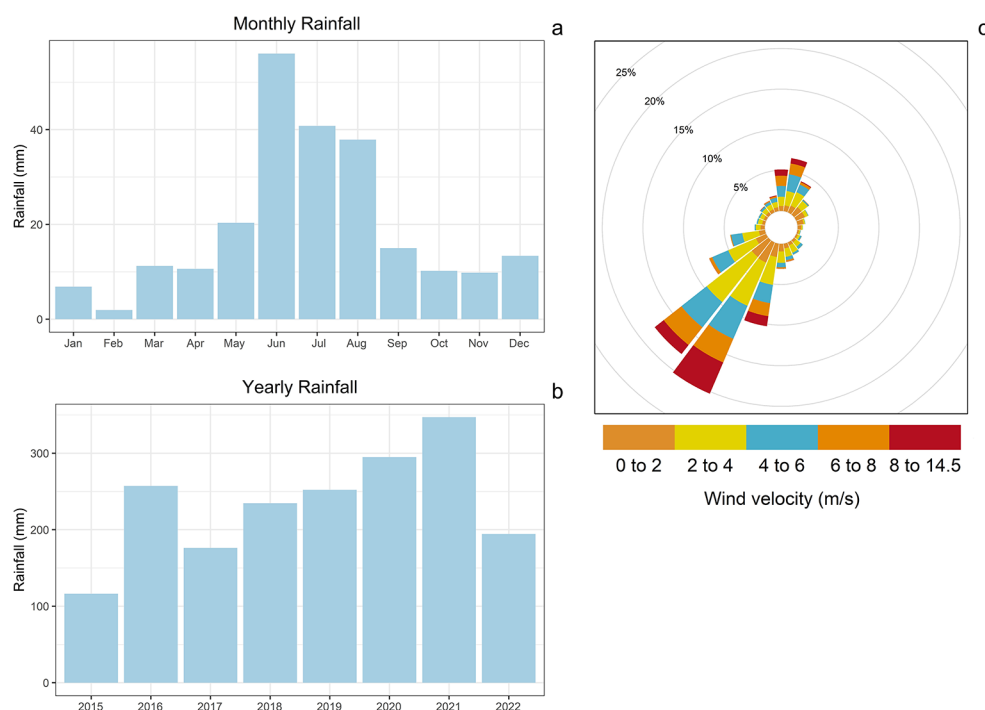


Fig. 2 The average monthly (a) and yearly rainfall (b) and the windrose (c) from 2015 to 2022 as measured by the climate station at Langebaanweg (Fig. 1) showing the dominating SW wind



Dust deposition monitoring

In addition to the $PM_{2.5}$ monitoring, seven dust buckets have been installed (Fig. 1). These buckets are named as follows: N-A (north-A), N-B (north-B), NE (northeast), CN (central-north), CS (central-south), SW (southwest), and SE (southeast). These buckets capture both the gravimetrically deposited and wet deposited dust, successfully used in, among others, Audoux et al. (2022) to determine the influence of cold pools on dust washout in the Sahel, Ganor and Foner (2001) for quantifying the yearly variation of dust deposition and the local contribution of the dust load over Israel, and Krahl et al. (2004) in the Okavango Delta in Botswana to determine the spatial variation of dust deposition and the possible origin of this dust. Other studies that used dust buckets successfully are McTainsh et al. (1997), where dust buckets were used to determine the input of dust into soils in Mali and the importance of locally derived dust in this process, and Rasmussen et al. (2018), which showed that dust deposition data are useful indicators for the indoor exposure to several elements. The advantages of these dust buckets are the low-cost and low-maintenance aspects of this equipment, which enables assessing the spatial variability. However, dust buckets can be contaminated by droppings or insects. There is furthermore a difference between the grain size distribution of the total suspended particles and the deposited particles, whereby deposited particles are expected to be larger on average (McTainsh et al. 1997), meaning that relating the dust deposition to the suspended particles should be done with caution.

The dust buckets were installed at a height of 2 to 3 m from the ground. The buckets were sampled approximately once a month (Table S1) and from the sample weight, the surface area of the dust buckets, and the sampling period, the depositional flux was calculated in $mg\ day^{-1}\ m^{-2}$. The equipment was installed from the beginning of 2015 until the end of 2022. Unfortunately, during the COVID-19 lockdown period from March 2020 until March 2022, the sampling interval was longer. Furthermore, over time, two dust buckets corroded (ARGOS 2022). Samples contaminated from bird droppings were excluded from further analyses.

National and international health standards for dust

To lower the negative effect of air pollution, the World Health Organisation (WHO) has set a guideline for a maximum average $PM_{2.5}$ concentration of $15\ \mu g\ m^{-3}$ daily and $5\ \mu g\ m^{-3}$ annually (WHO 2021). However, since 99% of the world's population lives above these guidelines (WHO 2021), the WHO has introduced four interim targets that offer a more gradual shift to lower air pollutant concentrations (WHO 2016, 2021). In addition, many nations have their own air quality standards (Vallack and Shillito 1998; You 2014; Kelly et al. 2017). South Africa has introduced the National Ambient Air Quality Standards (NAAQS) which prescribe a maximum average concentration of $PM_{2.5}$. Concerns for public health led to a change in the NAAQS: in 2030, the maximum daily average will be lowered from $40\ \mu g\ m^{-3}$ to $25\ \mu g\ m^{-3}$ and the maximum annual average will be lowered from $20\ \mu g\ m^{-3}$ to $15\ \mu g\ m^{-3}$ (DEA 2012).

South Africa has furthermore standards for the dust deposition flux described by the South African National Dust Control Regulations (DEA 2013). The standard for residential and light commercial areas is below $600 \text{ mg day}^{-1} \text{ m}^{-2}$ averaged over 30 days, but the Saldanha Bay Municipality has set $300 \text{ mg day}^{-1} \text{ m}^{-2}$ as a local goal (ARGOS 2022, 2023).

Data analyses and visualisation

The temporal change in daily $\text{PM}_{2.5}$ concentration and dust deposition flux was visualised using linear regression from the package “ggplot2” in R. To visualise the change in dust deposition flux, the date halfway through the sampling period has been used to plot the measured flux value. Additionally, due to the high measurement interval, a generalized additive mode smoothing with penalized regression was used for the daily average $\text{PM}_{2.5}$ concentration. This method was preferred over the local polynomial regression method due to the high number of data points. To determine and visualise the relationship between the dust deposition flux from the different stations and the $\text{PM}_{2.5}$ concentration, a correlation matrix was created with a Pearson correlation, using the package “corrplot” in R. To do so, the average of the $\text{PM}_{2.5}$ concentration was calculated over the sampling periods of the dust depositional fluxes. Due to the skewness of the data, the hourly and daily $\text{PM}_{2.5}$ concentrations might be non-parametric. For this reason, Wilcoxon tests (also called the Mann-Whitney test) were used to compare the value differences between the two sets. When multiple datasets were compared, ANOVA tests were utilised. For any statistical test, an alpha value of 0.01 was chosen to signify statistical significance. For boxplot graphs, values that are more than 1.5 times the interquartile range are visualised as separate data points.

To visualise the relationship between wind velocity, wind direction, and $\text{PM}_{2.5}$ concentration, polar plots were created using the package “openair” in R (Carslaw and Ropkins 2012). To create these plots, the hourly wind data from the Langebaanweg climate station was combined with the $\text{PM}_{2.5}$ data sampled at the same time. The lower sampling interval of the wind conditions means that not the whole $\text{PM}_{2.5}$ dataset was used to create the polar plots.

To determine which areas beyond the Saldanha Bay Municipality could be impacted by the dust, the Hybrid Single Particle Lagrangian Integrated Trajectory Model (HYSPPLIT, Stein et al. 2015; Rolph et al. 2017) was used to calculate the trajectory of particles from the port (Fig. 1). The trajectory was calculated for each day from 2015 to 2022 at 12:00 ($n=2557$). The trajectory was calculated for 120 h, with a starting height of 100 m, following the methods from Neff and Bertler (2015). For the weather

data, the Global Data Assimilation System (GDAS1) was used, a meteorological dataset that has a 3-hour interval and a 1-degree latitude-longitude grid. The location of the particles at 24 h and 120 h were visualised.

Results

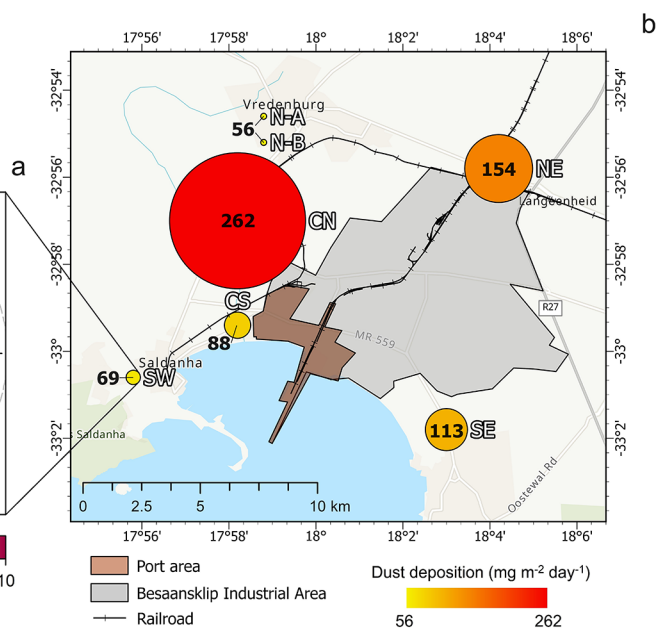
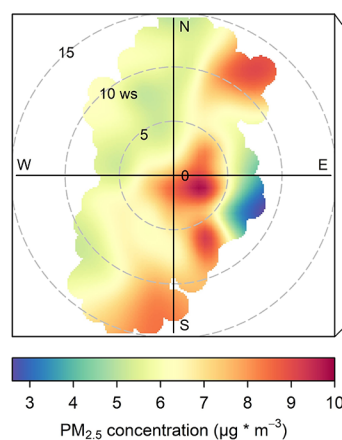
Spatial variation of dust deposition and origin of $\text{PM}_{2.5}$

The average dust deposition fluxes from 2015 to 2022 is $114 \text{ mg day}^{-1} \text{ m}^{-2}$, but the average over this period from the individual stations ranges between $56 \text{ mg day}^{-1} \text{ m}^{-2}$ and $262 \text{ mg day}^{-1} \text{ m}^{-2}$ (Fig. 3). The variation occurs within a 7.5 km radius, whereby the stations with the highest and lowest dust deposition flux are only 6 km away from each other. This illustrates the large spatial variability of dust fluxes in the region. The deposition fluxes are the smallest in the urban areas of Saldanha and Vredenburg ($69 \text{ mg day}^{-1} \text{ m}^{-2}$ and $56 \text{ mg day}^{-1} \text{ m}^{-2}$ respectively), and highest adjacent to the north-western part of the industrial area ($262 \text{ mg day}^{-1} \text{ m}^{-2}$). The areas close to the industrial region experience a generally higher dust deposition flux, except for the CS station west of the industrial area (Fig. 3).

The hourly measurements were used to create the polar plot of the $\text{PM}_{2.5}$ concentration in the town of Saldanha (Fig. 3). In total, most dust was brought by strong north-eastern and southern winds. This indicates that the industrial area is likely the origin of this dust, although no exact point of origin can be derived from this graph. Furthermore, a high dust concentration was associated with low wind speeds (below 2 m/s), which could indicate local dust sources such as traffic. The dust coming from the southeast to the southwest could originate from the coastal regions situated south and west of Saldanha (Fig. 1). The yearly resolved polar plots (Figure S4) show interannual variability in origin in the dust. Eastern dust sources dominated from 2016 to 2018, whereas dust from strong southern winds was most prominent in 2015.

Since the predominant wind direction is south to southwest, the dust emitted from the industrial area is most of the time not transported in the direction of the $\text{PM}_{2.5}$ monitoring in the town of Saldanha, but in the north- to northeastern direction (Fig. 1). It is therefore possible that the areas north to northeast of the port, such as the town of Vredenburg, have a higher $\text{PM}_{2.5}$ flux than the point where the $\text{PM}_{2.5}$ is being monitored. The measurement in Saldanha may therefore not capture the main transport of dust from the industrial area and might also not represent the highest health risk that the $\text{PM}_{2.5}$ emission poses.

Fig. 3 Polar plot for the $PM_{2.5}$ concentration from the monitoring station in the town of Saldanha from 2015 to 2018 (a) and the average dust deposition fluxes in $mg\ day^{-1}\ m^{-2}$ at the seven monitoring stations (b). The colour bar in the polar plot (a) indicates the $PM_{2.5}$ concentration related to certain wind speeds and wind directions, while the size and colour of the circles in the map (b) are an indication of the dust deposition flux



The large difference between the dust deposition at station CN, and N-A and N-B could be explained by the difference in elevation between these stations (Fig. 4). When sediment-carrying winds move over a hill, the dust deposition is strongest on the windward side and weakest at the peak (Goossens 1989, 2006; Zufall et al. 1999; Parker and Kinnersley 2004). This would explain the low dust deposition for stations N-A and N-B, considering their location on top of a hill, at 136 m (N-A) and 154 m (N-B) elevation, which is higher than station CN at 26 m elevation, but similar elevation as SE, NE, CS, and SW (Fig. 4).

Temporal variation of dust deposition

The dust deposition fluxes from the individual monitoring stations from 2015 to 2022 show a large variance (Fig. 5 and Figure S5). The median dust deposition increases over time ($R^2=0.19$) whereby the peak median dust deposition flux in 2022 is mainly driven by the high deposition flux at station SE which has been attributed to building activities within 100 m west of the measuring station (ARGOS 2023). The individual dust deposition fluxes from the monitoring stations and SE, SW, CS, and N-A show a weak, positive relationship with the year, which confirms the small increase in dust deposition over time, whereas CN and NE show no change ($R^2<0.01$) and N-B shows a weak decrease over time ($R^2=0.03$). There is furthermore no consistent seasonal trend in the dust deposition flux (Figure S6). The relationship between the different monitoring stations, the average deposition fluxes, the year, and the $PM_{2.5}$ concentration are shown in a Pearson correlation matrix (Figure S7). Dust deposition fluxes among the different stations are generally

weak but mostly positively correlated ($-0.08<r<0.72$). Surprisingly, the adjacent stations N-A and N-B showed no significant relationship with each other. This suggests that either the dust sources are local, or that additional drivers of dust transportation, such as elevation or influence from buildings in Vredenburg, drive a local imprint.

Temporal variation of $PM_{2.5}$

The average $PM_{2.5}$ concentration was $7.1\ \mu g\ m^{-3}$ reaching peak hourly concentrations of $95\ \mu g\ m^{-3}$ (Fig. 6a). The hourly values were transformed into daily average values to determine a temporal pattern (Fig. 6b). The daily average $PM_{2.5}$ concentration did show a weak decrease from 2015 to 2018. Per year, the daily concentration decreased significantly from 2017 to 2018 (Fig. 7a, $p=8.8\ *10^{-4}$), the other years the change was non-significant. A seasonal cycle in the $PM_{2.5}$ concentration can be discerned by a generalized additive mode smoothing regression (Sect. 2.4) whereby the $PM_{2.5}$ concentration peaks around winter and is lowest around mid-summer. The $PM_{2.5}$ concentration differed significantly (Fig. 7b, $p=0.006$) between summer (October to March) and winter (April to Sep) with an average concentration around 8% higher in winter. To understand the diurnal pattern of the $PM_{2.5}$ concentration, the time of the maximum daily $PM_{2.5}$ concentration was determined (Fig. 8a). The daily peak $PM_{2.5}$ concentration generally occurs between 06:00 and 09:00 and between 18:00 and 21:00. The difference in $PM_{2.5}$ between the high and the low concentration periods is statistically significant ($p<0.10^{-6}$) (Fig. 8b) and between 26% and 42% higher during the high concentration periods.

Fig. 4 Map of the elevation of the area and the location of the monitoring equipment, the towns, the roads and railroad, and the industrial area. Elevation data credits: NASA, USGS, SERVIR-RCMRD

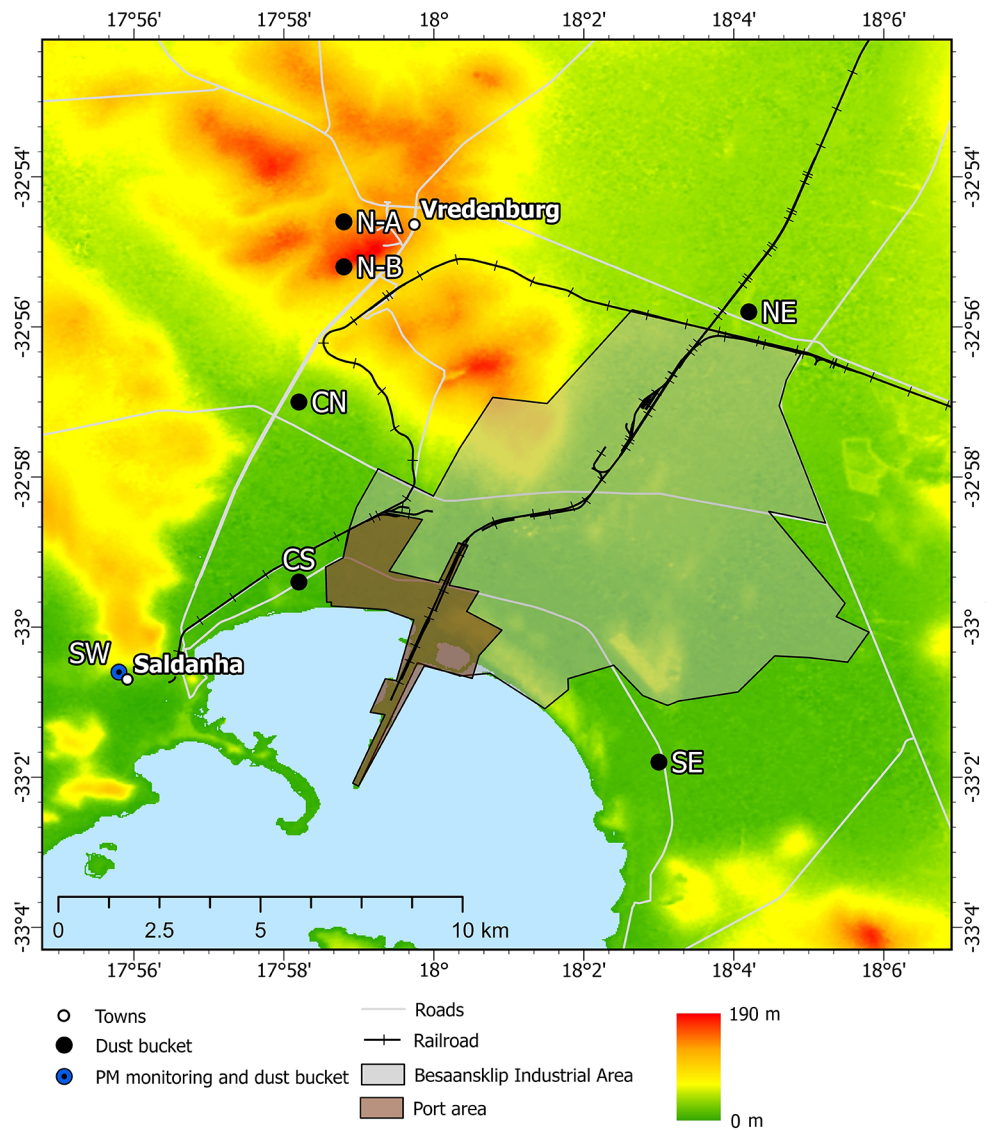
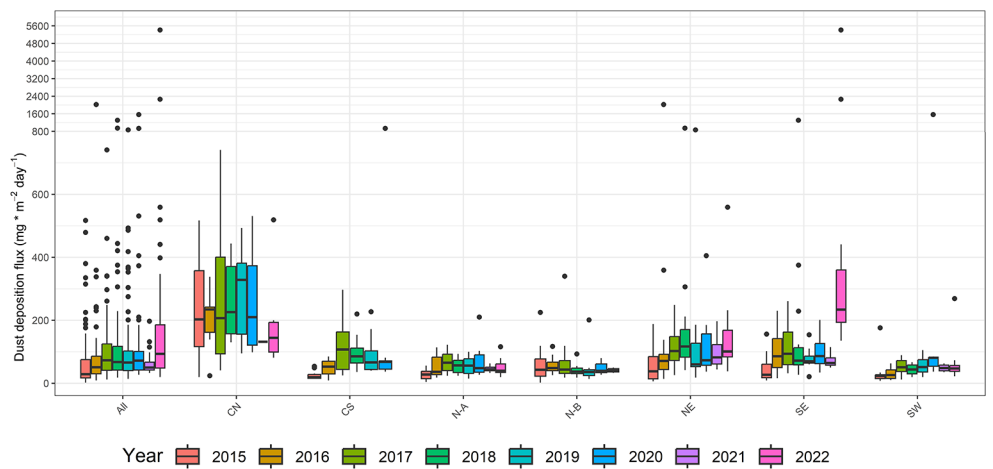


Fig. 5 The monthly dust deposition as measured by the individual monitoring station grouped per year. Note the break in the axis at 800 $\text{mg m}^{-2} \text{day}^{-1}$ to improve the visualisation of the outliers



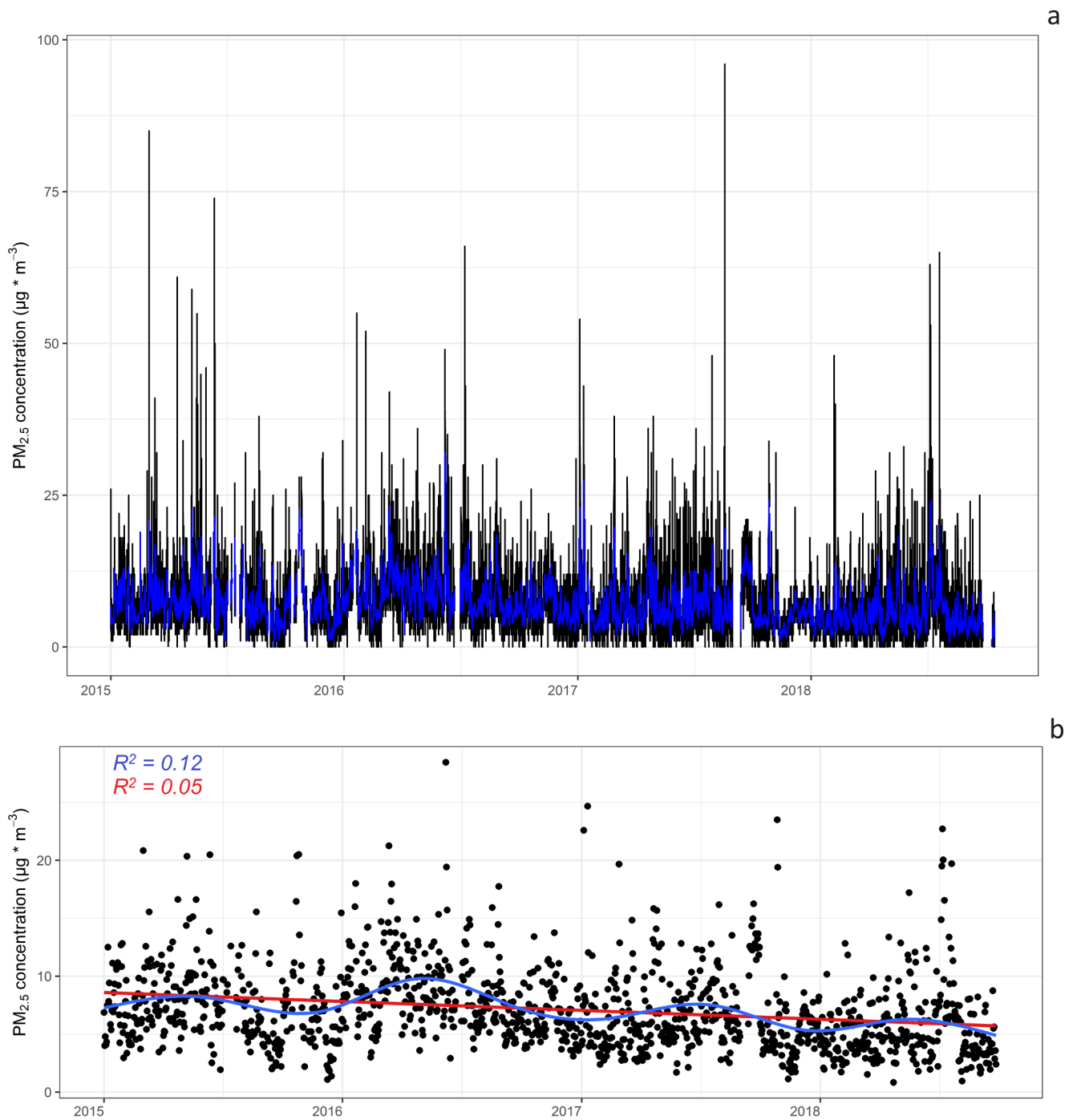


Fig. 6 PM_{2.5} concentrations illustrated as (a) measured hourly data (black line) and calculated 24-hour floating average (blue line), and (b) the calculated daily averages (black dots) with a generalized additive mode smoothing regression (blue line), and a linear regression (red line)

Fig. 7 Daily average $PM_{2.5}$ concentration for each year (a) and summer and winter (b). The diamond and the associated number reflect the average of the $PM_{2.5}$ concentration per group

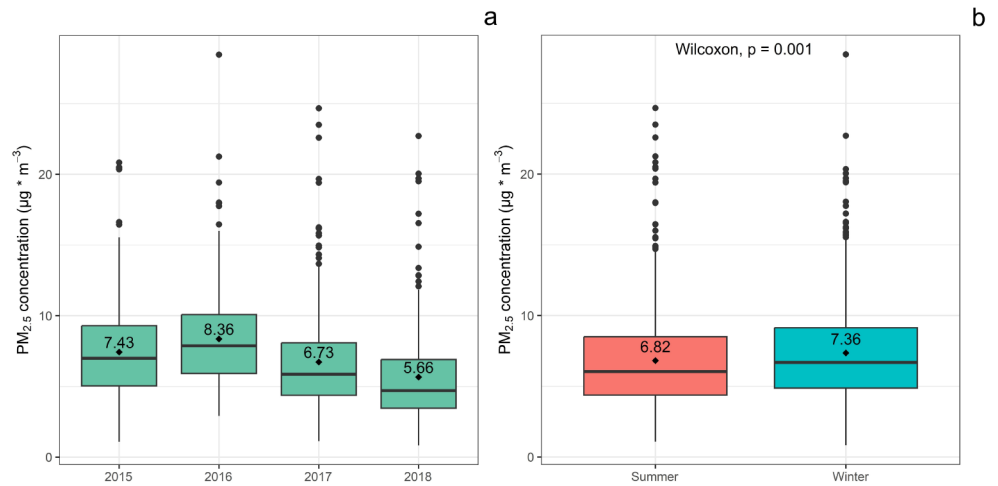
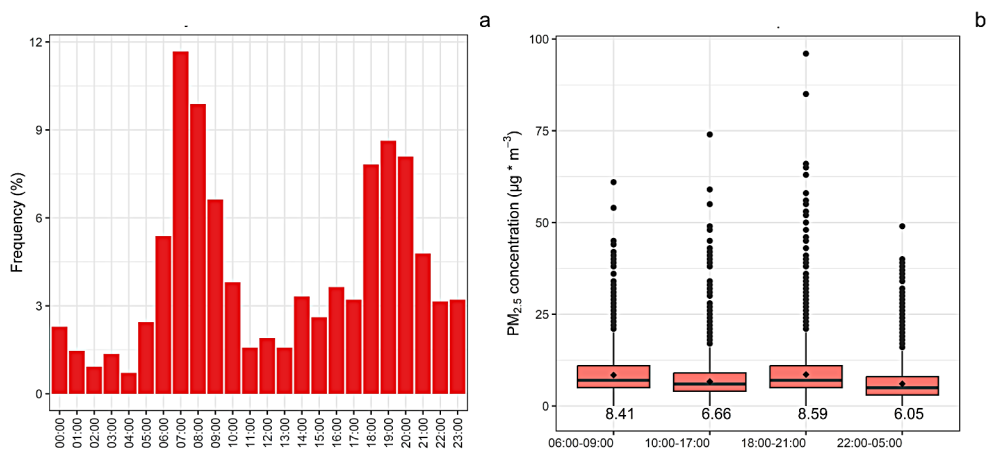


Fig. 8 Time of the day of peak concentration from the days between 2015–2018 (a), and averages of hourly $PM_{2.5}$ concentrations during different periods of the day. In (b), the diamond and the associated number reflect the average of the $PM_{2.5}$ concentration per group



The dust deposition fluxes did not show a significant correlation to the $PM_{2.5}$ concentrations ($-0.22 < r < 0.20$, Figure S7). This lack of a significant correlation is especially noteworthy at station SW ($r=0.002$) since $PM_{2.5}$ is measured at this location. This disconnect in the temporal pattern can also be observed in the difference in the seasonal pattern of the dust deposition and the $PM_{2.5}$ concentration, and the fact that the $PM_{2.5}$ concentration shows a small decrease over time, whereas the dust deposition flux shows a small increase.

Rainfall impact

There is a strong significant difference in the $PM_{2.5}$ concentration on hours with and without rain ($p < 2 * 10^{-16}$) whereby the average is 54% higher for days without rain (Fig. 9a). However, there is no correlation between the hourly rainfall and $PM_{2.5}$ concentration ($R^2 < 0.01$, Fig. 9b). The rainfall amount did furthermore not correlate with any of the dust deposition fluxes observed at the seven monitoring stations ($r < 0.2$, Figure S7).

Discussion

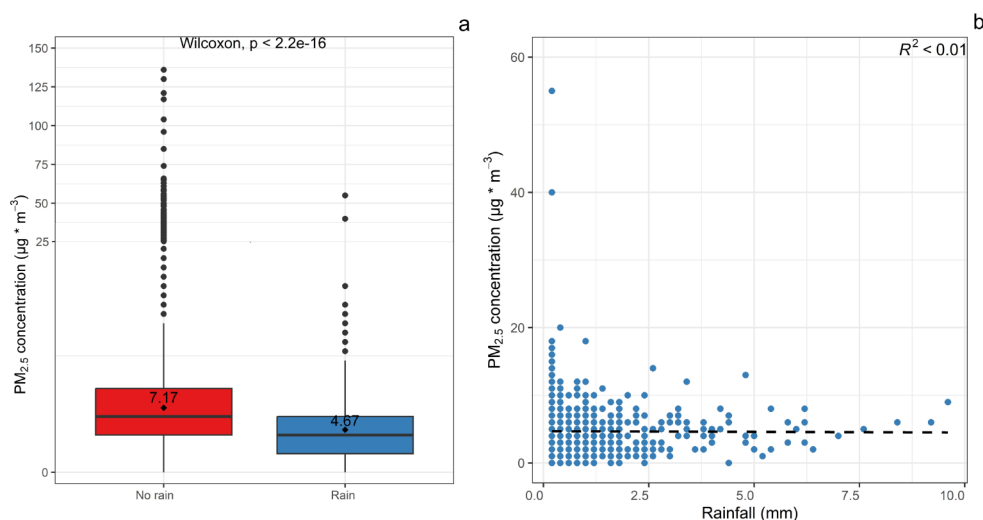
Spatiotemporal variation and controls of dust

Spatial

The $PM_{2.5}$ particles captured at the Saldanha monitoring station, southwest of the industrial area, have a predominant northeastern to eastern origin (Fig. 3), which corresponds to the location of the industrial area, although an exact point source cannot be identified. Furthermore, a southwestern transport likely carried particles originating from the coastal regions in 2015 (Figure S4). Such coastal regions are commonly recognised sources of aerosols, including emissions of sea spray and mineral dust from sandy beaches and dune areas (e.g. Engelbrecht et al. 2009; Dansie et al. 2017). In addition, the high concentration related to a low wind speed could indicate emissions from local sources such as traffic or construction sites.

Determining the driver of dust deposition is more difficult. Relating the spatial variability of the dust deposition fluxes to certain wind events or wind conditions remains

Fig. 9 The average daily $PM_{2.5}$ concentration of day with and without rain whereby the squares and the number describes the average of the total values (a) and the relationship between the daily $PM_{2.5}$ concentration and rainfall (b)



challenging due to the low sampling interval, as dust deposition was only assessed monthly. The highest dust deposition fluxes were measured at the monitoring station located north of the port (CN) and northwest of the industrial area and railway (NE) (Fig. 3). This is in line with the $PM_{2.5}$ particles at Saldanha that originate from the direction of the port and the industrial area and the southern wind direction transporting a majority of the particles in a northern direction. Besides proximity to the industrial source, elevation (in the case of N-A and N-B) and local dust sources caused by construction (for SE in 2022) influenced the dust deposition.

Inter-annual

Despite the increase in industrial activities around the port, both the $PM_{2.5}$ concentration and the dust deposition flux showed no significant increase over time. In fact, the daily $PM_{2.5}$ concentration decreased significantly from 2017 to 2018 (Fig. 7). The cause of this decrease in measured $PM_{2.5}$ per year is difficult to attribute to certain industrial activities. Rainfall appears to have a strong influence on the daily $PM_{2.5}$ concentration, but since the wettest year is also the year with the highest average $PM_{2.5}$ concentration, this effect appears to not be dominating on longer timescales.

Seasonal

The $PM_{2.5}$ concentration and the dust deposition flux show only weak seasonal fluctuations (Figs. 5 and 6, and 7). Slightly higher dust concentrations were observed in winter possibly due to the typical north-to-northeast winter winds (Figure S1). These winds would transport suspended particles from the industrial area to the $PM_{2.5}$ monitoring station located to the southwest, resulting in a higher wintertime $PM_{2.5}$ concentration. The dust deposition, in contrast, did not show any consistent seasonal trend.

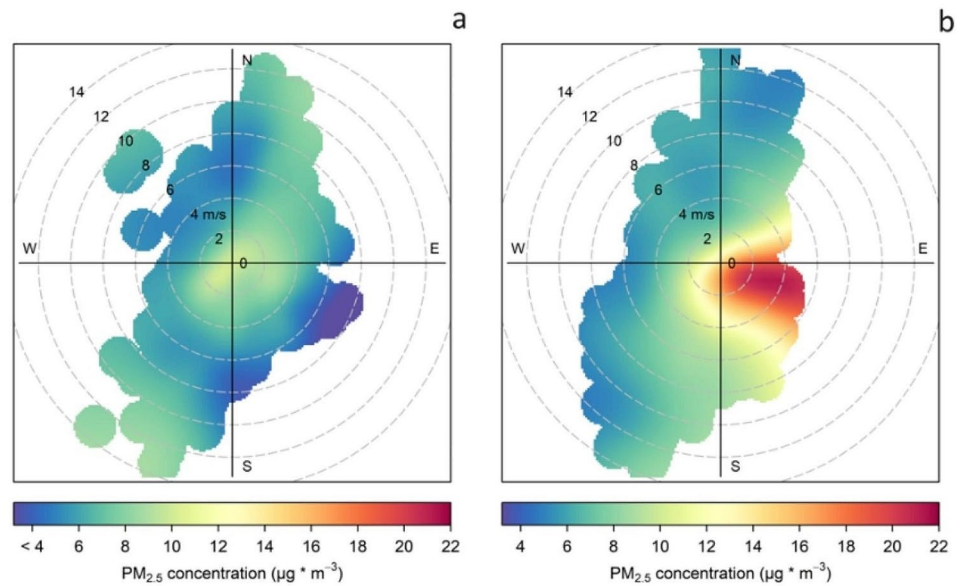
Diurnal

Peak dust concentration occurred in the morning and the evening, which could be caused by high emissions and/or favourable wind conditions. Windroses indicate that wind velocities are typically low in the morning and higher in the afternoon and evening (Figure S8). Hereby, the weaker morning winds tend to originate from both the southeastern and northern winds, whereas in the evening, southeastern winds dominate. Polar plots determined for the morning hours between 07:00 to 09:00 and evening hours between 18:00 to 20:00 point to differences in source areas: the highest dust concentration in the morning occurs when there is less wind, which suggests the dust originates from local sources near the measuring station, such as traffic (Fig. 10a), whereas in the evening, the highest dust concentration occurs when there are eastern winds, which suggests the dust originates from the industrial area (Fig. 10b). The higher emission in the afternoon could be related to higher activity during this time since the wind in the evening is dominantly from the southwest. This shift in emissivity could be confirmed by increasing the spatial resolution of $PM_{2.5}$ concentration measurements.

Rainfall

The daily $PM_{2.5}$ concentration is related to days with and without rainfall, which could be interpreted as a consequence of the wet removal effect of rain (Liu et al. 2020; Zhao et al. 2020). This relationship is, however, more complex as the rainfall amount is unrelated to $PM_{2.5}$ concentration, even though both rainfall and low $PM_{2.5}$ concentrations can be associated with strong northern winds (Figure S9). It is furthermore surprising that rainfall appears not to influence dust deposition (Figure S7, $r < 0.2$). This goes against the generally assumed importance of wet deposition, as

Fig. 10 The polar plots of the hourly data for the morning between 07:00 to 09:00 (a), and evening between 18:00 to 20:00 (b). These times were chosen based on the periods of highest measured $PM_{2.5}$ concentrations



described in several studies that use dust buckets (Ganor and Foner 2001; Krahl et al. 2004; Morales-Baquero et al. 2013; Audoux et al. 2022). However, these studies mainly propose the importance of wet deposition for finer particles (PM_{10}) whereas larger particles seemed to be less affected by rainfall, which could explain the relationship of rainfall with the daily $PM_{2.5}$ concentration and the lack of relationship with dust deposition. We therefore postulate that the fact that $PM_{2.5}$ is related to days with rainfall is a consequence of air masses originating from the Atlantic Ocean carrying low dust loads. This demonstrates the complex and dynamic influence of meteorological conditions on dust transport and deposition.

Summary of the spatiotemporal variability and controls

Interannual changes and trends of $PM_{2.5}$ and dust deposition were largely lacking significance despite the progressive extension of industrial activities, but seasonal changes were apparent. Winter has on average an 8% higher $PM_{2.5}$ concentration than summer. In addition, diurnal fluctuations occurred, with higher $PM_{2.5}$ concentrations in the afternoon and evening than in the morning. The polar plots show that certain wind directions and velocities carry more dust, a relationship that fluctuates during the day. Wind and rainfall patterns explain the inter-annual, seasonal, and diurnal variability of $PM_{2.5}$ and dust deposition in the area to a certain extent. For example, days without rain have 54% higher $PM_{2.5}$ concentration compared to days with rain. Furthermore, a low $PM_{2.5}$ concentration measured was associated with southwestern to northern winds with a velocity above 4 m s^{-1} . The low dust loads of air masses originating from the Atlantic Ocean are also evident considering that the

lowest concentration of $PM_{2.5}$ in the Saldanha Bay area is observed during strong (above 6 m s^{-1}) western to northwestern winds. In contrast, the highest $PM_{2.5}$ concentration occurred in conditions of weak (below 2 m s^{-1}) and strong (above 10 m s^{-1}) winds from the northeast. However, such meteorological conditions could not explain the $PM_{2.5}$ and dust distribution entirely. Additionally, these dynamics appear to be affected by the complexity and diversity of dust emitted in these industrial areas, including traffic, as well as small-scale factors such as the elevation of the sampling sites.

Monitoring improvements

The dust buckets-based monitoring in the study area offers an affordable opportunity to assess spatial variability. However, there appears to be no significant correlation between the dust deposition fluxes measured monthly at the seven dust bucket stations and the $PM_{2.5}$ concentrations for the same period. This is not in line with the general assumption that there is a significant relationship between the total suspended particle concentration and the $PM_{2.5}$ and PM_{10} concentrations (Tucker 2000; Bacon et al. 2011; Zhang et al. 2017). However, this disconnect between deposition fluxes and suspended particles has been observed previously in dust events over Israel from 1969 to 1995 (Ganor and Foner 2001). Around Saldanha Bay, this lack of relationship could be explained by the difference in the particle size assessed by the dust buckets and $PM_{2.5}$ sensor. The deposited dust could include larger particles, such as silt and fine sand and point to mineral sources even if the emission is due to local anthropogenic activities, while the fine particle ($PM_{2.5}$) concentration could predominantly be associated with

combustion and industrial activities (Saucy et al. 2018; Ji et al. 2018; Cui et al. 2019). Despite the merit of dust buckets as cheap, sustainable measurement methods for understanding the composition of dust, dust buckets do not selectively capture the finer particles which are the general indicators of the risks to public health.

So far, only one fine particle sensor has been used in this study. Understanding the high spatiotemporal variation of $PM_{2.5}$ in urban and industrial environments is challenging with such a limited number of $PM_{2.5}$ measurements (Petavratzi et al. 2005; Zhang et al. 2018). Therefore, an important next step for the improvement in the understanding of the origin of dusts and the associated health risks, and developing mitigation strategies, would be to establish a higher spatial resolution network of $PM_{2.5}$ measurements. The recent developments of low-cost sensors enable such high-resolution measurements (Pope et al. 2018; Awokola et al. 2022) and the spatial variability assessed through dust bucket dust deposition data has informed about the key sites for future fine particle sensor sites. It should be noted that these sensor data are not flawless: they only represent a specific fraction (typically $PM_{2.5}$ or PM_{10}), and the measurements can be disturbed by changes in humidity and larger fraction particles (Stavroulas et al. 2020; Barkjohn et al. 2021). Satellite imagery methods (Yu and Zahidi 2023) and physical models in combination with computational techniques (Zhang et al. 2018) could be explored as an addition to the regular dust monitoring in the Saldanha Bay area. Lastly, real-time inhalation monitoring needs to be included for accurate health impact assessment (Khamraev et al. 2021), as well as the chemical composition of the particles, especially considering that industrial and mining dust often includes potentially toxic components.

Potential impact

Public health impact

The initial goal of the monitoring activities was to determine whether the air quality in the residential areas adhered to the national air standard. The municipality's dust deposition standard of $300 \text{ mg day}^{-1} \text{ m}^{-2}$ is exceeded 8.6% of the time between 2015 and 2022 and the recommendation by the South African National Dust Control Regulations for residential areas of $600 \text{ mg day}^{-1} \text{ m}^{-2}$ is exceeded 2.1% of the time (Fig. 5). The daily average $PM_{2.5}$ concentrations remain far below the daily NAAQS of $40 \text{ } \mu\text{g m}^{-3}$, and the $PM_{2.5}$ annual average remains below the NAAQS of $20 \text{ } \mu\text{g m}^{-3}$. Even the stricter health standard envisaged for 2030 ($25 \text{ } \mu\text{g m}^{-3}$ daily, and $15 \text{ } \mu\text{g m}^{-3}$ annually), which is comparable to the 2nd interim target set by the WHO, is only exceeded one day during the four years of monitoring.

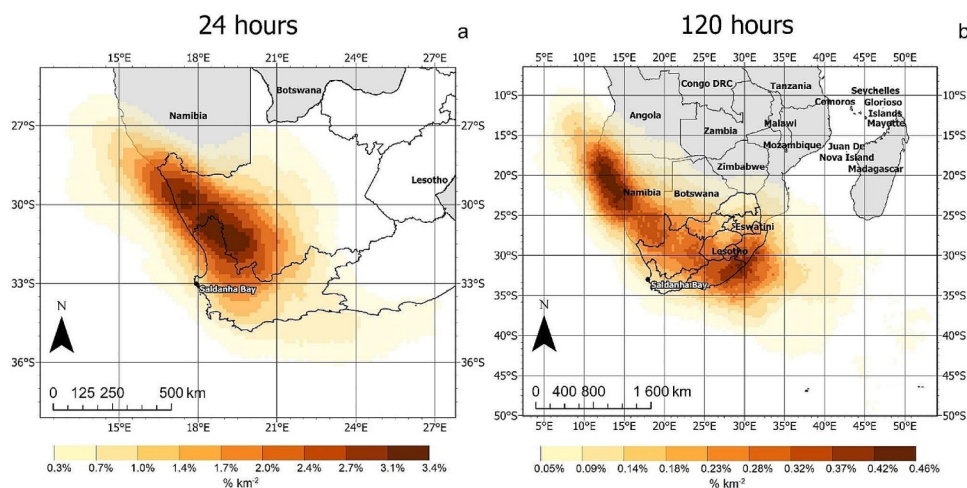
The current WHO daily air quality standard of $15 \text{ } \mu\text{g m}^{-3}$ $PM_{2.5}$ was exceeded 2.9% of the days (ca. 10 days per year). The WHO standard for a yearly average $PM_{2.5}$ concentration of $5 \text{ } \mu\text{g m}^{-3}$, is exceeded every year, including when considering the annual floating average of the $PM_{2.5}$ concentration. However, comparing this to the WHO global air quality dataset (WHO 2024), Saldanha belongs to the lowest 10% areas in $PM_{2.5}$ concentration. Despite the relatively low concentration, exposure to a daily average $PM_{2.5}$ concentration of $7.1 \text{ } \mu\text{g m}^{-3}$ could be associated with a mortality increase of approximately 0.5–5% (Schwartz et al. 2002; Shi et al. 2016).

To understand the precise health effects of the industrial area in the Saldanha Bay municipality, it should be considered that the dust deposition data and the polar plots show that the location of the $PM_{2.5}$ monitoring station may not receive the highest dust concentration. The dust-bucket data informed that to improve the understanding of the high-risk area, it would be necessary to place $PM_{2.5}$ monitoring equipment closer to the dust plume source. It is likely that these areas receive higher dust concentrations and that these regions should be the leading areas in determining the threat of these industries on public health.

Environmental impact

Besides the impact on public health, the impact on the environment should be considered. As mentioned in the introduction, this can both be a fertilizing effect of the dust (Peterson et al. 1993; Okin et al. 2011; Moore et al. 2013; Dansie et al. 2017; Barkley et al. 2019) and a toxic effect, especially in the case of anthropogenic dust (Farmer 1993; Griffin and Kellogg 2004; Paytan et al. 2009). These effects can be regional, but dust particles also have the potential to travel far distances. The HYSPLIT model shows the location density of the particles 24 h and 120 h after suspension (Fig. 11). These figures reveal that especially the area northwest of Saldanha Bay (e.g., most of the West Coast and Namakwa Districts) is affected by the dust from Saldanha Bay within 24 h after suspension (Fig. 11a). The trajectories 120 h are characterised by a redistribution between particles transported further north, along the west coast of Namibia, and particles transported to the southeast, over South Africa and to the Indian Ocean (Fig. 11b). The location of each individual run is shown in Figure S10 and shows that there are days when particles have the potential to reach as far as the Australian or Antarctic continents. These trajectories indicate that both the impact on land and the ocean need to be considered to fully understand the impact of the dust. To further assess the potential consequences of the dust on the environment, the geochemistry, solubility, and presence of any toxic particles need to be analysed.

Fig. 11 The density of the particles emitted daily from the industrial hub of Saldanha Bay from 2015 to 2022 calculated by the HYSPLIT trajectory modeling. The figures show the spatial distribution of the trajectories after 24 h (a) and 120 h (b) of suspension



Conclusion

The $PM_{2.5}$ concentration has been monitored from 2015 to 2018 in the town of Saldanha, and the dust deposition flux has been monitored from 2015 to 2022 at seven different locations surrounding the Saldanha Bay industrial area. Despite changes in industrial activities, there have been only small changes in the annual dust deposition and $PM_{2.5}$ concentration. Most of the diurnal and seasonal variation in $PM_{2.5}$ can be attributed to a certain extent to wind and rain conditions, but there remains a large variability unexplained. It appeared furthermore challenging to identify a single source of dust, which demonstrated the complexity of dust emission from a diverse industrial area. The $PM_{2.5}$ concentration remained below the national standard and the envisaged standard of 2030. However, the current monitoring does not provide insight into the air pollution in high-risk areas and would need improvement to better assess the public health risks.

Supplementary Information The online version contains supplementary material available at <https://doi.org/10.1007/s11869-024-01581-8>.

Acknowledgements This work is based on the research supported in part by the National Research Foundation of South Africa (Grant Numbers CPRR150612119375, SRUG2204204036, and MESA170607237905) awarded to PI Dr Susanne Fietz. The weather data has been provided by the South African Weather Service (SAWS).

Author contributions All authors contributed to the study's conception and design. Material preparation and data collection were performed by René Toesie and Grant Ravenscroft and the analyses of data were performed by Kaukuraee I. Kanguuehi and Heleen C. Vos. The first draft of the manuscript was written by Heleen C. Vos and all authors commented on previous versions of the manuscript. All authors read and approved the final manuscript.

Funding This work is based on the research supported in part by the National Research Foundation of South Africa (Grant Numbers CPRR150612119375, SRUG2204204036, and MESA170607237905)

awarded to PI Dr Susanne Fietz.

Open access funding provided by Stellenbosch University.

Data availability The datasets generated during the current study are available in the Saldanha Bay Municipality repository: <https://sbm.gov.za/environmental/>. The hourly meteorological data from 2015 to 2022 is available at <https://zenodo.org/records/10926062>.

Declarations

Ethics approval and consent to participate Not applicable.

Consent for publication Not applicable.

Competing interests The authors declare no competing interests.

Open Access This article is licensed under a Creative Commons Attribution 4.0 International License, which permits use, sharing, adaptation, distribution and reproduction in any medium or format, as long as you give appropriate credit to the original author(s) and the source, provide a link to the Creative Commons licence, and indicate if changes were made. The images or other third party material in this article are included in the article's Creative Commons licence, unless indicated otherwise in a credit line to the material. If material is not included in the article's Creative Commons licence and your intended use is not permitted by statutory regulation or exceeds the permitted use, you will need to obtain permission directly from the copyright holder. To view a copy of this licence, visit <http://creativecommons.org/licenses/by/4.0/>.

References

- AEC (2022) The state of Saldanha Bay and Langebaan Lagoon 2021/2022. Anchor Environmental Consultants, Cape Town
- Al-Swadi HA, Usman ARA, Al-Farraj AS et al (2022) Sources, toxicity potential, and human health risk assessment of heavy metals-laden soil and dust of urban and suburban areas as affected by industrial and mining activities. *Sci Rep* 12:8972. <https://doi.org/10.1038/s41598-022-12345-8>
- ARGOS (2022) Test Report: Dust Fallout Monitoring. Saldanha Bay Municipality, <https://sbm.gov.za/environmental/>
- ARGOS (2023) Test Report: Dust Fallout Monitoring. Saldanha Bay Municipality, <https://sbm.gov.za/environmental/>

- Audoux T, Laurent B, Marticorena B et al (2022) Wet deposition fluxes of Mineral Dust and their relation with Cold pools in the Central Sahel. *Geophys Res Lett* 49. <https://doi.org/10.1029/2021GL095005>. e2021GL095005
- Awokola B, Okello G, Johnson O et al (2022) Longitudinal ambient PM_{2.5} measurement at fifteen locations in eight sub-saharan African countries using low-cost sensors. *Atmosphere* 13:1593. <https://doi.org/10.3390/atmos13101593>
- Bacon SN, McDonald EV, Amit R et al (2011) Total suspended particulate matter emissions at high friction velocities from desert landforms. *J Geophys Research: Earth Surf* 116. <https://doi.org/10.1029/2011JF001965>
- Barkjohn KK, Gantt B, Clements AL (2021) Development and application of a United States-wide correction for PM_{2.5} data collected with the PurpleAir sensor. *Atmos Meas Tech* 14:4617–4637. <https://doi.org/10.5194/amt-14-4617-2021>
- Barkley AE, Prospero JM, Mahowald N et al (2019) African biomass burning is a substantial source of phosphorus deposition to the Amazon, Tropical Atlantic Ocean, and Southern Ocean. *Proceedings of the National Academy of Sciences* 116:16216–16221. <https://doi.org/10.1073/pnas.1906091116>
- Bauer SE, Im U, Mezuman K, Gao CY (2019) Desert Dust, Industrialization, and agricultural fires: Health impacts of Outdoor Air Pollution in Africa. *J Geophys Research: Atmos* 124:4104–4120. <https://doi.org/10.1029/2018JD029336>
- Bridges EM, Oldeman LR (1999) Global Assessment of Human-Induced Soil Degradation. *Arid Soil Res Rehabil* 13:319–325. <https://doi.org/10.1080/089030699263212>
- Carslaw DC, Ropkins K (2012) Openair — an R package for air quality data analysis. *Environ Model Softw* 27–28:52–61. <https://doi.org/10.1016/j.envsoft.2011.09.008>
- Csavina J, Landázuri A, Wonaschütz A et al (2011) Metal and Metalloid contaminants in Atmospheric aerosols from Mining Operations. *Water Air Soil Pollut* 221:145–157. <https://doi.org/10.1007/s11270-011-0777-x>
- Csavina J, Field J, Taylor M et al (2012) A review on the importance of metals and metalloids in Atmospheric Dust and Aerosol from Mining Operations. *Sci Total Environ* 433:58–73. <https://doi.org/10.1016/j.scitotenv.2012.06.013>
- Cui M, Lu H, Wiggs GFS et al (2019) Quantifying the effect of geomorphology on aeolian dust emission potential in northern China. *Earth Surf Proc Land* 44:2872–2884. <https://doi.org/10.1002/esp.4714>
- Dansie AP, Wiggs GFS, Thomas DSG, Washington R (2017) Measurements of windblown dust characteristics and ocean fertilization potential: the ephemeral river valleys of Namibia. *Aeolian Res* 29:30–41. <https://doi.org/10.1016/j.aeolia.2017.08.002>
- DEA (2012) National Ambient Air Quality Standard for Particulate Matter with Aerodynamic Diameter Less Than 2.5 Micron Metres (PM_{2.5}). Department of Environmental Affairs (DEA)
- DEA (2013) National Environmental Management: Air Quality Act, 2004. Department Of Environmental Affairs
- DEA&DP (2019) Risk and Resilience Assessment of Natural Capital in the Greater Saldanha Bay Municipality: A Navigational Tool for Strategic-Level decision-making. Western Cape Department of Environmental Affairs and Development Planning, Cape Town
- Engelbrecht JP, McDonald EV, Gillies JA et al (2009) Characterizing Mineral dusts and other Aerosols from the Middle East—Part I: ambient sampling. *Inhalation Toxicol* 21:297–326. <https://doi.org/10.1080/08958370802464273>
- Entwistle JA, Hursthouse AS, Reis PAM, Stewart AG (2019) Metalliferous Mine Dust: Human Health impacts and the potential determinants of Disease in Mining communities. *Curr Pollution Rep* 5:67–83. <https://doi.org/10.1007/s40726-019-00108-5>
- Farmer AM (1993) The effects of dust on vegetation—a review. *Environ Pollut* 79:63–75. [https://doi.org/10.1016/0269-7491\(93\)90179-R](https://doi.org/10.1016/0269-7491(93)90179-R)
- Ganor E, Foner HA (2001) Mineral dust concentrations, deposition fluxes and deposition velocities in dust episodes over Israel. *J Geophys Research: Atmos* 106:18431–18437. <https://doi.org/10.1029/2000JD900535>
- Ginoux P, Prospero JM, Gill TE et al (2012) Global-scale attribution of anthropogenic and natural dust sources and their emission rates based on MODIS Deep Blue aerosol products. *Rev Geophys* 50:3005. <https://doi.org/10.1029/2012RG000388>
- Goossens D (1989) Height distortion and the sedimentation of dust on topographic scale models: considerations and simulations. *Earth Surf Proc Land* 14:655–667. <https://doi.org/10.1002/esp.3290140619>
- Goossens D (2006) Aeolian deposition of dust over hills: the effect of dust grain size on the deposition pattern. *Earth Surf Proc Land* 31:762–776. <https://doi.org/10.1002/esp.1272>
- Goudie AS (2013) Desert dust and human health disorders. *Environ Int* 63 C:101–113. <https://doi.org/10.1016/j.envint.2013.10.011>
- Grantz DA, Garner JHB, Johnson DW (2003) Ecological effects of particulate matter. *Environ Int* 29:213–239. [https://doi.org/10.1016/S0160-4120\(02\)00181-2](https://doi.org/10.1016/S0160-4120(02)00181-2)
- Griffin DW, Kellogg CA (2004) Dust storms and their impact on Ocean and Human Health: Dust in Earth's atmosphere. *Eco-Health* 1:284–295. <https://doi.org/10.1007/s10393-004-0120-8>
- Ji X, Yao Y, Long X (2018) What causes PM_{2.5} pollution? Cross-economy empirical analysis from socioeconomic perspective. *Energy Policy* 119:458–472. <https://doi.org/10.1016/j.enpol.2018.04.040>
- Kelly JT, Reff A, Gantt B (2017) A method to predict PM_{2.5} resulting from compliance with national ambient air quality standards. <https://doi.org/10.1016/j.atmosenv.2017.05.009>. *Atmospheric Environment* 162:
- Khamraev K, Cheriyan D, Choi J (2021) A review on health risk assessment of PM in the construction industry – current situation and future directions. *Sci Total Environ* 758:143716. <https://doi.org/10.1016/j.scitotenv.2020.143716>
- Khreis H, Sanchez KA, Foster M et al (2023) Urban policy interventions to reduce traffic-related emissions and air pollution: a systematic evidence map. *Environ Int* 172:107805. <https://doi.org/10.1016/j.envint.2023.107805>
- Koch D, Bond TC, Streets D et al (2007) Global impacts of aerosols from particular source regions and sectors. *J Geophys Research: Atmos* 112. <https://doi.org/10.1029/2005JD007024>
- Krah M, McCarthy TS, Annegarn H, Ramberg L (2004) Airborne dust deposition in the Okavango Delta, Botswana, and its impact on landforms. *Earth Surf Proc Land* 29:565–577. <https://doi.org/10.1002/esp.1051>
- Kristensen LJ, Taylor MP, Morrison AL (2015) Lead and zinc dust depositions from ore trains characterised using lead isotopic compositions. *Environ Sci: Processes Impacts* 17:631–637. <https://doi.org/10.1039/C4EM00572D>
- Landrigan PJ, Baker EL (1981) Exposure of children to heavy metals from smelters: Epidemiology and toxic consequences. *Environ Res* 25:204–224. [https://doi.org/10.1016/0013-9351\(81\)90090-6](https://doi.org/10.1016/0013-9351(81)90090-6)
- Li X-D, Jin L, Kan H (2019) Air pollution: a global problem needs local fixes. *Nature* 570:437–439. <https://doi.org/10.1038/d41586-019-01960-7>
- Liu Z, Shen L, Yan C et al (2020) Analysis of the influence of precipitation and wind on PM_{2.5} and PM₁₀ in the atmosphere. *Adv Meteorol* 2020:1–13
- Mahowald NM, Albani S, Kok JF et al (2014) The size distribution of desert dust aerosols and its impact on the Earth system. *Aeolian Res* 15:53–71. <https://doi.org/10.1016/j.aeolia.2013.09.002>
- Marcella MP, Eltahir EAB (2014) The role of mineral aerosols in shaping the regional climate of West Africa. *J Geophys Research: Atmos* 119:5806–5822. <https://doi.org/10.1002/2012JD019394>
- McCartor A, Becker D (2010) Top six toxic threats, world's worst pollution problems report. Blacksmith Institute, New York

- McTainsh GH, Nickling WG, Lynch AW (1997) Dust deposition and particle size in Mali, West Africa. *CATENA* 29:307–322. [https://doi.org/10.1016/S0341-8162\(96\)00075-6](https://doi.org/10.1016/S0341-8162(96)00075-6)
- Moore CM, Mills MM, Arrigo KR et al (2013) Processes and patterns of oceanic nutrient limitation. *Nat Geosci* 6:701–710. <https://doi.org/10.1038/ngeo1765>
- Morales-Baquero R, Pulido-Villena E, Reche I (2013) Chemical signature of Saharan dust on dry and wet atmospheric deposition in the south-western Mediterranean region. *Tellus B: Chem Phys Meteorol* 65:18720. <https://doi.org/10.3402/tellusb.v65i0.18720>
- Neff PD, Bertler NAN (2015) Trajectory modeling of modern dust transport to the Southern Ocean and Antarctica. *J Geophys Res: Atmos* 120:9303–9322. <https://doi.org/10.1002/2015JD023304>
- Okin GS, Baker AR, Tegen I et al (2011) Impacts of atmospheric nutrient deposition on marine productivity: roles of nitrogen, phosphorus, and iron. *Glob Biogeochem Cycles* 25. <https://doi.org/10.1029/2010GB003858>
- Pan B, Wang Y, Hu J et al (2018) Impacts of Saharan Dust on Atlantic Regional Climate and implications for Tropical cyclones. *J Clim* 31:7621–7644. <https://doi.org/10.1175/JCLI-D-16-0776.1>
- Pandey A, Brauer M, Cropper ML et al (2021) Health and economic impact of air pollution in the States of India: the global burden of Disease Study 2019. *Lancet Planet Health* 5:e25–e38. [https://doi.org/10.1016/S2542-5196\(20\)30298-9](https://doi.org/10.1016/S2542-5196(20)30298-9)
- Parker ST, Kinnnersley RP (2004) A computational and wind tunnel study of particle dry deposition in complex topography. *Atmos Environ* 38:3867–3878. <https://doi.org/10.1016/j.atmosenv.2004.03.046>
- Paytan A, Mackey KRM, Chen Y et al (2009) Toxicity of atmospheric aerosols on marine phytoplankton. *Proc Natl Acad Sci* 106:4601–4605. <https://doi.org/10.1073/pnas.0811486106>
- Petavratzi E, Kingman S, Lowndes I (2005) Particulates from mining operations: a review of sources, effects and regulations. *Miner Eng* 18:1183–1199. <https://doi.org/10.1016/j.mineng.2005.06.017>
- Peterson BJ, Deegan L, Helfrich J et al (1993) Biological responses of a Tundra River to Fertilization. *Ecology* 74:653–672. <https://doi.org/10.2307/1940794>
- Pope P F, Gichuru M, Ng'ang'a D et al (2018) Airborne particulate matter monitoring in Kenya using calibrated low-cost sensors. *Atmos Chem Phys* 18:15403–15418. <https://doi.org/10.5194/acp-18-15403-2018>
- Querol X, Tobias A, Pérez N et al (2019) Monitoring the impact of desert dust outbreaks for air quality for health studies. *Environ Int* 130:104867. <https://doi.org/10.1016/j.envint.2019.05.061>
- Rasmussen PE, Levesque C, Chénier M, Gardner HD (2018) Contribution of metals in resuspended dust to indoor and personal inhalation exposures: relationships between PM10 and settled dust. *Build Environ* 143:513–522. <https://doi.org/10.1016/j.buildenv.2018.07.044>
- Ritchie H, Roser M (2019) Outdoor Air Pollution. *Our World in Data*
- Rolph G, Stein A, Stunder B (2017) Real-time Environmental Applications and Display sYstem: READY. *Environ Model Softw* 95:210–228. <https://doi.org/10.1016/j.envsoft.2017.06.025>
- Salawu-Rotimi A, Lebre P, Vos HC et al (2021) Gone with the wind: Microbial communities Associated with Dust from Emission Farmlands. *Microb Ecol* 1–11. <https://doi.org/10.1007/s00248-021-01717-8>
- Saldanha Bay Municipality (2023) First Review and Amendment of the 5th Generation Integrated Development Plan 2022–2027. Saldanha Bay Municipality
- Samset BH, Sand M, Smith CJ et al (2018) Climate impacts from a removal of Anthropogenic Aerosol emissions. *Geophys Res Lett* 45:1020–1029. <https://doi.org/10.1002/2017GL076079>
- Saucy A, Rössli M, Künzli N et al (2018) Land Use Regression Modelling of Outdoor NO₂ and PM_{2.5} concentrations in three low income areas in the Western Cape Province, South Africa. *Int J Environ Res Public Health* 15:1452. <https://doi.org/10.3390/ijerph15071452>
- Schwartz JD, Laden F, Zanobetti A (2002) The concentration-response relation between PM_{2.5} and daily deaths. *Environ Health Perspect* 110:1025–1029. <https://doi.org/10.1289/ehp.021101025>
- SEP (2021) Socio-Economic Profile: Saldanha Bay Municipality. Western Cape Government
- Shi L, Zanobetti A, Kloog I et al (2016) Low-concentration PM_{2.5} and mortality: estimating Acute and Chronic effects in a Population-based study. *Environ Health Perspect* 124:46–52. <https://doi.org/10.1289/ehp.1409111>
- Stavroulas I, Grivas G, Michalopoulos P et al (2020) Field evaluation of low-cost PM sensors (Purple Air PA-II) under Variable Urban Air Quality conditions, in Greece. <https://doi.org/10.3390/atmos11090926>. *Atmosphere* 11:
- Stein AF, Draxler RR, Rolph GD et al (2015) NOAA's HYSPLIT Atmospheric transport and dispersion modeling system. *Bull Am Meteorol Soc* 96:2059–2077. <https://doi.org/10.1175/BAMS-D-14-00110.1>
- Tucker WG (2000) An overview of PM_{2.5} sources and control strategies. *Fuel Process Technol* 65–66:379–392. [https://doi.org/10.1016/S0378-3820\(99\)00105-8](https://doi.org/10.1016/S0378-3820(99)00105-8)
- Vallack HW, Shillito DE (1998) Suggested guidelines for deposited ambient dust. *Atmos Environ* 32:2737–2744. [https://doi.org/10.1016/S1352-2310\(98\)00037-5](https://doi.org/10.1016/S1352-2310(98)00037-5)
- WHO (2016) Ambient air pollution: a global assessment of exposure and burden of disease. World Health Organization, Geneva
- WHO (2021) WHO global air quality guidelines: particulate matter (PM_{2.5} and PM₁₀), ozone, nitrogen dioxide, sulfur dioxide and carbon monoxide. World Health Organization, Geneva
- WHO (2024) WHO global ambient air quality database (update 2024). World Health Organization: Geneva, Switzerland
- Xia W, Wang Y, Chen S et al (2022) Double trouble of Air Pollution by Anthropogenic Dust. *Environ Sci Technol* 56:761–769. <https://doi.org/10.1021/acs.est.1c04779>
- You M (2014) Addition of PM_{2.5} into the National Ambient Air Quality standards of China and the contribution to Air Pollution Control: the Case Study of Wuhan, China. *Sci World J* 2014:768405. <https://doi.org/10.1155/2014/768405>
- Yu H, Zahidi I (2023) Environmental hazards posed by mine dust, and monitoring method of mine dust pollution using remote sensing technologies: an overview. *Sci Total Environ* 864:161135. <https://doi.org/10.1016/j.scitotenv.2022.161135>
- Zhang X-X, Sharratt B, Chen X et al (2017) Dust deposition and ambient PM₁₀ concentration in northwest China: spatial and temporal variability. *Atmos Chem Phys* 17:1699–1711. <https://doi.org/10.5194/acp-17-1699-2017>
- Zhang G, Rui X, Fan Y (2018) Critical review of methods to Estimate PM_{2.5} concentrations within specified Research Region. *ISPRS Int J Geo-Information* 7. <https://doi.org/10.3390/ijgi7090368>
- Zhao X, Sun Y, Zhao C, Jiang H (2020) Impact of precipitation with different intensity on PM_{2.5} over typical regions of China. <https://doi.org/10.3390/atmos11090906>. *Atmosphere* 11:
- Zheng N, Liu J, Wang Q, Liang Z (2010) Health risk assessment of heavy metal exposure to street dust in the zinc smelting district, Northeast of China. *Sci Total Environ* 408:726–733. <https://doi.org/10.1016/j.scitotenv.2009.10.075>
- Zufall MJ, Dai W, Davidson CI (1999) Dry deposition of particles to wave surfaces: II. Wind tunnel experiments. *Atmos Environ* 33:4283–4290. [https://doi.org/10.1016/S1352-2310\(99\)00178-8](https://doi.org/10.1016/S1352-2310(99)00178-8)